Lepidosomes acquire fluorescence after encystation: Including additional notes of morphological events during encystation and reconsideration of the morphological features in the ciliate *Colpoda cucullus*

Yoichiro Sogame [1,*], Ryota Saito [1], Tatsuya Sakai [1], Taiga Shimizu [1], Taiki Ono [1], Ryota Koizumi [1], Kaito Mizumachi [2]

[1] National institute of Technology Fukushima Callage, 30 Nagao Kamiarakawa Taira Iwaki Fukushima, 970-8034 Japan.
[2] Laboratory of Marine Biology, Faculty of Science and Technology, Kochi University, Kochi 780-8520, Japan.
*Corresponding author: Yoichiro Sogame; E-mail: sogame@fukushima-nct.ac.jp

ABSTRACT

The resting cyst formation (encystment) is a survival strategy against environmental stressors, and is found in many species of single-celled eukaryotic organisms. The process incorporates cell differentiation accompanied by drastic morphological changes. This study presents observation via fluorescence microscopy on the encystation process of *Colpoda cucullus*. We confirmed that *C. cucullus*, which was identified by 18S rRNA analysis, contains lepidosomes, which are cyst-specific cell structures. The existence of these structures in *Colpoda* species is controversial at present, so we present background information concerning the controversy. Moreover, we reveal that lepidosomes acquire autofluorescence after formation, that is, encysting cells contain lepidosomes lacking autofluorescence while mature cysts contain lepidosomes exhibiting autofluorescence. In addition, we describe the process of formation of nuclear surrounding particles (NSPs), which are cyst-specific cell structures.

Keywords: *Colpoda*, cyst, *cryptobiosis*, lepidosome, autofluorescence

INTRODUCTION

The survival of microorganisms depends on their ability to sense changes in the environment and respond to new situations (Gutiérrez et al., 2003). Encystment is a common occurrence among free-living ciliates, which often undergo this process under adverse environmental conditions (Verni and Rosati, 2011). Encystment represents a strategy against various environmental stressors such as starvation (Gutiérrez et al., 2001), desiccation (Taylor and Stickland, 1936), freezing (Uspenskaya and Lozina-Lozinski, 1979), high and low temperatures (Taylor and Stickland, 1936), ultraviolet irradiation (Uspenskaya and Lozina-Lozinski, 1979; Matsuoka et al., 2017), and acidity (Sogame et al., 2011). Therefore, an important part of the life cycle of most ciliates is the formation of resting cysts (Benčaťová and Tirjaková, 2018).

The process of encystment in the ciliate genus *Colpoda* was reported to be controlled by an intracellular signaling pathway (Matsuoka et al., 2010) triggered by an increase in intracellular Ca^{2+} concentration caused by Ca^{2+} inflow (Sogame and Matsuoka, 2013), which leads to protein phosphorylation (Sogame et al., 2012a) and alteration of protein expression (Izquierdo et al., 2000; Chessa et al., 2002; Sogame et al., 2012b, 2014). It also involves progressive and drastic morphological changes (Gutiérrez et al.,2003). The morphological events during the encystment process of *Colpoda cucullus* have been described and include mitochondrial fragmentation, expulsion of net-like globules, synthesis of ectocysts and endocysts, and chromatin extrusion (Funatani et al., 2010). The net-like globules (Foissner 1993) were defined as lepidosomes (Foissner et al., 2003) and are reported to have autofluorescence (Matsuokaet al., 2017). The main scope of this study was to reveal whether lepidosomes acquire fluorescence after their formation. In addition, nuclear surrounding particles (NSPs) were previously reported to be cyst-specific fluorescent materials surrounding the nucleus (Matsuoka et al., 2017); however, details on their formation have not yet been elucidated. We observed the NSP formation process by double visualization (nuclei were visualized with Propidium Iodide (PI) staining and NSPs were visualized by their autofluorescence) by fluorescence microscopy.

As stated above, the *C. cucullus* cysts in our culture cell line (*C. cucullus* R2TTYS) expelled lepidosomes. However, *C. cucullus* was previously reported to contain no lepidosomes (Foissner, 1993), although *C. cucullus* Nag-1, whose partial 18S rRNA sequence is closest to that of *C. lucida*, was reported to have lepidosomes (Funadani et al., 2016). Another aim of this study was to reconsider the presence of lepidosomes as a taxonomic characteristic of *C. cucullus*.

MATERIALS AND METHODS
Cell culture
Colpoda cucullus R2TTYS was cultured in an infusion of dried wheat leaves supplemented with bacteria (*Klebsiella pneumoniae* NBRC13277 strain) as food. *K. pneumoniae* was cultured on agar plates containing 1.5% agar, 0.5% polypeptone, 0.5% yeast extract, and 0.5% NaCl.

Human liver adenocarcinoma cell line SK-HEP-1cells were kindly provided from Prof. T. Nakatsura and Dr. M. Shimomura in National Cancer Center, Japan. The cells were cultured in Dulbecco's Modified Eagle's Medium (DMEM, Sigma-Aldrich Japan LLC., Tokyo, Japan) supplemented with 10% fetal bovine serum, 1% L-glutamine, 1% penicillin, and 1% streptomycin for 3–4 days.

Encystment induction
Encystment was induced according to Sogame et al., 2019. The cultured vegetative cells were corrected by centrifugation (1500 g, 1min) and suspended at high cell density (> 10,000 cells/mL) in encystment-inducing medium [1 mM Tris-HCl (pH 7.2), 0.1 mM CaCl$_2$].

Microscopy

Vegetative cells, cysts, and dry cysts were observed using the Avart A1 system (Carl Zeiss Microscopy Co., Ltd., Tokyo, Japan; Fig. 1 A-1, A-3) or Axio Scope A1 system (Carl Zeiss Microscopy Co., Ltd.; Fig. 1 A-2).

To visualize lepidosomes, cysts at 6 h ('immature cysts', Fig. 2 A-1, 2B a1–a3, 2C 'Immature cysts') and more than 1 week ('mature cysts', Fig. 2 A-2, 2B b1–b3, 2C 'Mature cysts') after the onset of encystment induction were stained with Congo Red solution [0.25% Congo Red in 1mM Tris-HCl (pH 7.2) (Fig. 2)] for 30 min, washed with 1 mM Tris-HCl (pH 7.2) (Fig. 2A), and observed under an optical microscope (Axio Scope A1; Fig. 2A) or a confocal laser microscope (FluoView 10i, Olympus Corporation, Tokyo, Japan; Fig. 2B) using a PI filter (emission maximum, 620 nm) to visualize Congo Red fluorescence (Fig. 2B a-2, b-2, 2C '620 nm') or DAPI filter (emission maximum, 460 nm) to visualize autofluorescence (Fig. 2B a-1, a-2, 2C '460 nm') with 405 nm and 473 nm laser diode (LD) excitation peaks. The rates of fluorescing cells were directly calculated under the confocal laser microscope. The significance of differences among samples was evaluated prepared by the Mann-Whitney U test.

For 4′,6-diamidino-2-phenylindole (DAPI) and propidium iodide (PI) double staining (Fig. 3), SK-HEP-1 cells (for control), *Colpoda* vegetative cells, and *Colpoda* cysts were prepared following two protocols (short-fix protocol and long-fix protocol) as follows. In the short-fix protocol, cells were fixed by 2% (final concentration) paraformaldehyde in Phosphate buffered saline (PBS) for 5 min, washed with PBS, and suspended in 1% (final concentration) NP40 in PBS for 1 h. Second, in the long-fix protocol, cells were fixed by 2% (final concentration) paraformaldehyde in PBS for 1 week, washed with PBS, and suspended in 1% (final concentration) NP40 in PBS for 1 h. Subsequently during both protocols, the cells were washed with PBS and stained with DAPI (final concentration 0.001%) and PI (final concentration 0.002%) in PBS for 15 min, and observed using a confocal laser microscope with a DAPI filter (emission maximum, 460 nm) with 405 nm LD excitation peak and PI filter (emission maximum, 620 nm) with 473-nm LD excitation peak.

For double-visualization of nuclei by PI staining and NSPs (Fig. 4), cells were stained with PI following a long staining protocol and subsequently observed by a confocal laser microscope under a DAPI filter (emission maximum, 460 nm) to visualize autofluorescence, and a PI filter (emission maximum, 620 nm) to visualize PI fluorescence with 473-nm LD excitation peak.

## Amplification and sequencing of 18S rRNA and phylogenetic analysis

Total genomic DNA was extracted from *C. cucullus* R2TTYS using the DNeasy Blood and Tissue Kit (Qiagen K. K., Tokyo, Japan) according to the manufacturer's instructions. Polymerase chain reaction (PCR) amplification for the partial 18S rRNA gene (1623 base-pairs, bp) was performed using the genomic DNA as a template. The PCR product was purified with a PCR Clean-Up Kit (Nippon Gene CO. LTD, Japan) and sequenced via BigDye Terminator v3.1 Cycle Sequencing Kit analyzed on a 3730 xl DNA analyzer (Thermo Fisher Scientific K. K., Tokyo, Japan). The primer sets has been previously described (Funadani et al., 2016). The nucleotide sequence was assembled using CLC Main

Workbench software (Filgen Inc., Aichi, Japan), and was used to search International Nucleotide Sequence Database Collaboration (INSDC). The sequence determined in this study have been deposited in INSFC under accession numbers LC441007. The estimation of the best evolutionary model and construction of a neighbor-joining (NJ) tree using the T92 model (Tamura, 1992) were performed in MEGA 6.0 (Tamura et al., 2013). A sequence of *Cyrtolophosis mucicola* (EU039898.1) was used as outgroup. The tree probability was assessed using bootstrap resampling of 1000 replicates.

RESULTS AND DISCUSSION

The vegetative cells, cysts, and dry cysts of our culture cell line of *C. cucullus* R2TTYS are shown in Fig. 1A. The partial nucleotide sequence of the 18S rRNA gene in our strain (LC441007/INSDC) was 99% the same as that in *C. cucullus* EU039893.1 (1620/1623 bp), *C. cucullus* Nag-1 strain AB918716.1 (1591/1601 bp), *C. inflata* PABBc-30 strain KJ60798.1 (1615/1623 bases), and *C. lucida* EU039895.1 (1609/1622 bp). The NJ tree showed that the partial sequence of 18S rRNA gene of the strain was most closely related to that of *C. cucullus* EU0398983.1 (Fig. 1B); we therefore identified our culture cell line as *C. cucullus*. However, it seemed that the cysts of the *C. cucullus* R2TTYS strain expelled small particles outside the cyst wall (Fig. 1A-2), which appeared to be lepidosomes (Foissner et al., 2005); the presence of lepidosomes disagrees with a previous report on *C. cucullus* (Foissner, 1993). To identify whether the expelled particles were lepidosomes, immature cysts (i.e., 6 h after the onset of encystment) and mature cysts (i.e., more than 1 week after the onset of encystment) were stained with Congo Red and observed by optical microscopy, because lepidosomes are reported to be visibly stained by this dye (Funadani et al., 2016). The observations (Fig. 2A) indicated that the *C. cucullus* R2TTYS strain expelled lepidosomes around their cyst wall. This result agreed with reports of *C. cucullus* Nag-1 strain (Funadani et al., 2016), *C. inflata* (Foissner, 1993), and *C. lucida* (Foissner, 1993), but disagreed with that of the *C. cucullus* strain reported by Foissner (1993). Molecular phylogenetic analysis showed that the partial sequence of the 18S rRNA gene of *C. cucullus* R2TTYS was most closely related to that of *C. cucullus* EU0398983.1 (Fig. 1B), although the *C. cucullus* R2TTYS strain contained lepidosomes. A previous study reported that *C. cucullus* Nag-1, which does have lepidosomes, was most closely related to *C. lucida*, although its morphological features agreed with those of *C. cucullus* in a 1993 report by Foissner (Funadani et al., 2019). These results suggest the possibility that lepidosomes are an intraspecific variation or that *C. lucida* might actually be a synonymic relationship of *C. cucullus*.

(A)
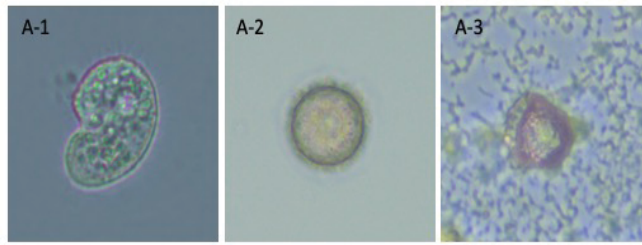
(B)
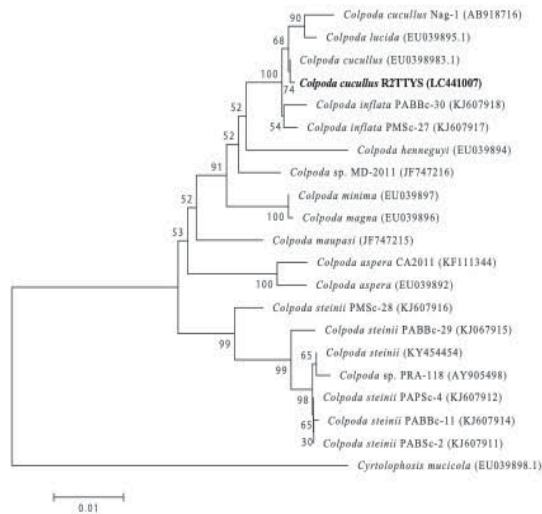
Fig. 1. Optical microscopy analysis and phylogenetic analysis of *C. cucullus* R2TTYS used in this study. (A) Optical microscopy images: vegetative cell (A-1), 1-week-old cyst (A-2), and dry cyst (A-3). The scale bar represents 20 µm. (B) Neighbor-joining (NJ) tree of the species of *Colpoda*, which was constructed by partial 18S rRNA gene sequences (1623 bp). The scale indicates genetic distance of T92 model. Numbers near the internal branches are percentage of bootstrap value. The bold letter shows haplotype of strain of *C. cucullus* R2TTYS determined in this study. The accession number of each sequence is indicated in parentheses.
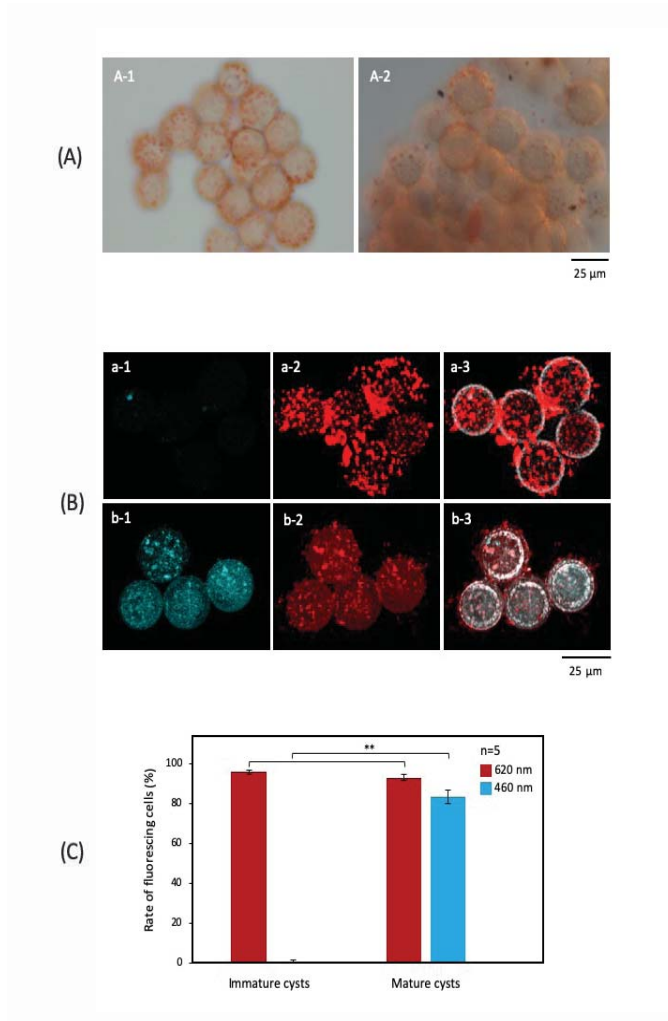
Fig. 2. Congo Red staining of encystation (at 6 h; A-1) and more than 1-week-old cysts (A-2) observed by optical microscopy. The scale bar represents 25 μm. Observation of lepidosomes by confocal laser microscopy (B). Observation of lepidosomes of encysting cell (a) and 1-week-old cysts (b). They were stained with Congo Red. Detection of autofluorescence of lepidosomes (a-1, b-1), fluorescence of Congo Red (b-2, b-3), and merged bright field images (a-3, b-3). The scale bar represents 25 μm. The rates of fluorescing cysts were calculated (C). Cysts 6 h after the onset of encystment induction 'Immature cysts' and more than 1 week after the onset of encystment induction 'Mature cysts' were stained with Congo Red and detected autofluorescence at an emission maximum of 460 nm '460 nm' and fluorescence of Congo Red at an emission maximum of 620 nm '620 nm', respectively. Columns and bars correspond to the means and their standard errors, respectively, of five measurements. Double asterisks indicate significant differences among columns at p < 0.01 (Mann-Whitney U test).

According to a previous report (Matsuoka et al., 2017), lepidosomes of mature cysts exhibit autofluorescence. In this study we found new information about lepidosomes. Indeed, the lepidosomes of mature cysts exhibited autofluorescence (Fig. 2B b-1); however, lepidosomes of immature cysts did not show autofluorescence (Fig. 2B a-1). To further clarify this, we prepared a double visualization of lepidosomes, that is, Congo Red-stained lepidosomes were visualized by both autofluorescence (at a wavelength of 460 nm) and fluorescence from Congo Red (at a wavelength of 620 nm). Congo Red staining can be observed with excitation (Clement and Truong, 2014). Our observations showed that lepidosomes in cells during encystation showed fluorescence at a wavelength of 620 nm (Fig. 2B a-2) but not at an emission maximum of 460 nm (Fig. 2B a-1). We confirmed the existence of lepidosomes in cells during encystation, however they did not show autofluorescence. In contrast, the fluorescence of lepidosomes in mature cysts was detected at both 620 nm (Fig. 2B b-2) and 460 nm (Fig. 2B b-1). Overlaying showed that the two types of fluorescence almost merged (Fig. 2B b-3). Subsequently, the rate of cysts which emitted fluorescence were confirmed (Fig 2C). In immature cysts, 96.1 % of cysts emitted fluorescence at a wavelength of 620 nm but only 1.0 % of cysts emitted fluorescence at a wavelength of 460 nm (Fig 2C 'Immature cysts'). On the other hand, 93.2 % and 83.4 % of cysts emitted fluorescence at a wavelength of 620 nm and 460 nm, respectively in mature cysts (Fig 2C 'Mature cysts'). The rate of fluorescing cells by Congo Red staining (fluorescence at a wavelength of 620 nm) of immature cysts was almost same as much as it of mature cysts ($p > 0.05$), however, the rate of autofluorescing (fluorescence at a wavelength of 460 nm) cells of immature cysts was significantly lower than that of mature cysts ($p < 0.01$). These results indicated that lepidosomes are produced in the early phase of the encystment process and acquire fluorescence later in the process.

In addition to lepidosomes, NSPs have also been reported as fluorescent structures of cysts (Matsuoka et al., 2017); however, detailed information about the formation process of NSPs has not been elucidated. However, we revealed the process of NSP formation in relation to the positions of nuclei (Fig. 4). NSPs were visualized as autofluorescence (emission maxima, 460 nm) and nuclei were stained with PI and observed at an emission maximum of 620 nm. The double visualization was performed using a general PI staining protocol (short-fix protocol; see Materials and Methods), however, nuclei were not stained with PI− (Fig. 3C 'S-PI'). To find the cause of the result, double staining of nuclei with DAPI and PI was performed. In consequence, nuclei in both *Colpoda* vegetative cells (Fig. 3B 'S-DAPI') and cysts (Fig. 3C 'S-DAPI') were stained with DAPI although both of them were not stained with PI (Fig. 3B, 3C 'S-PI'). Hence, PI was ineffective in both *Colpoda* vegetative cells (Fig. 3B 'S-PI') and cysts (Fig. 3C 'S-PI'). On the other hand, the fluorescent signals of DAPI (Fig. 3A 'S-DAPI') and PI (Fig. 3A 'S-PI') were almost co-localized in SK-HEP-1 cells via the same protocol (Fig. 3A 'S-Merge'). By extending the fixation time, the DAPI fluorescence in *Colpoda* vegetative cells (Fig. 3B 'L-DAPI') and cysts (Fig. 3C 'L-DAPI') and that of PI in *Colpoda* vegetative cells (Fig. 3B 'L-PI') and cysts (Fig. 3C 'L-PI') were co-localized in both *Colpoda* vegetative cells (Fig. 3B 'L-Merge') and cysts (Fig. 3C 'L-Merge'), respectively. Nevertheless, the long-fix protocol was problematic in SK-HEP-1 cells (Fig. 3A 'L-Merge'). In this case, PI did not work (Fig. 3A 'L-PI') although DAPI was

effective (Fig. 3A 'L-DAPI'). Since PI and DAPI bind strongly to DNA, nuclei must be stained with them if they got inside of cells and nuclei by surfactant preparation. PI was possibly trapped by cell structure or substances outside of nuclei because nuclei were apparently darkened (Fig. 3C 'S-PI').− Unfortunately, we cannot explain why PI did not work in *Colpoda* cells, but we were at least able to establish a staining protocol. Then, vegetative cells and cysts at 3 h, 6 h, 9 h, 12 h, 1 d, 3 d, 1 week, 2 weeks, and 3 weeks after the onset of encystment induction were prepared by long-fix protocol and double visualization was performed. The nuclei of all cells were stained with PI and the NSP formation process revealed the positional relationship between nuclei and NSPs (Fig. 4). At 12 h after the onset of encystment induction, a phenomenon which appeared to be chromatin extrusion (Akematsu and Matsuoka, 2008) occurred and the NSPs began to form around the nuclei (Fig. 4, 12 h, arrowhead). Thereafter, NSPs were gradually formed around the macro- and micronuclei. The photos shown as Fig. 4 were representative from repeated experiments, and the time course of NSP formation was similar among the repeated experiments.
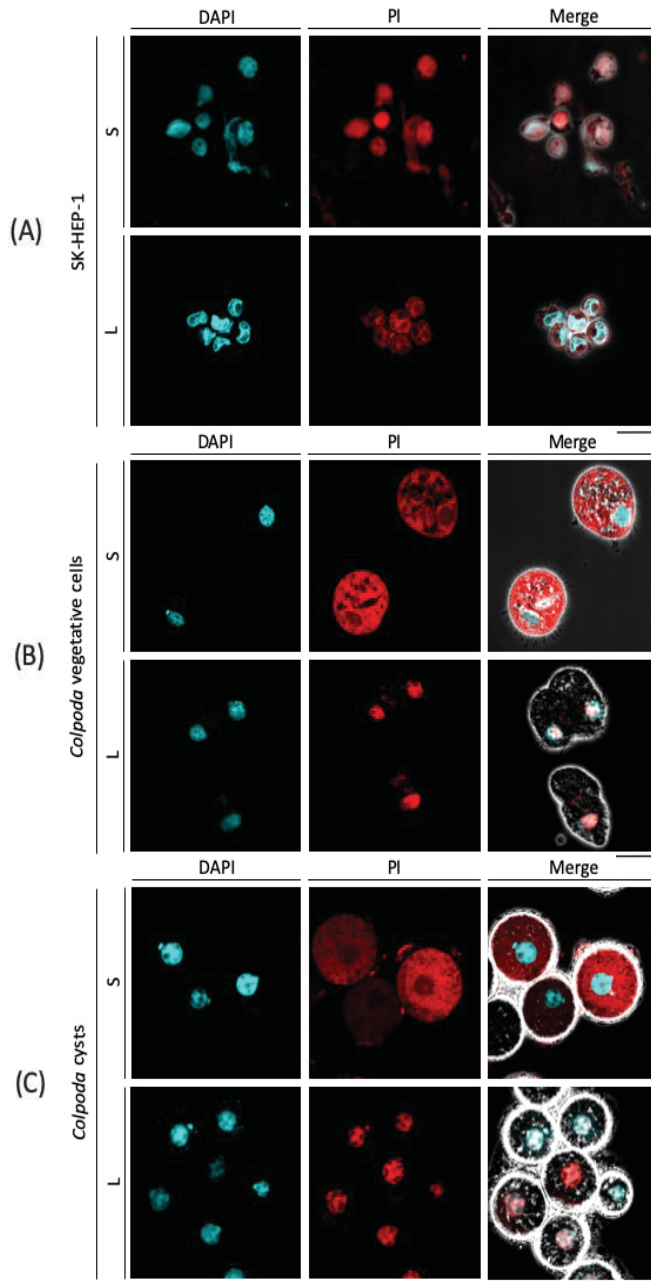
Fig. 3. Images of double staining. SK-HEP-1 cells (A), *Colpoda* vegetative cells (B), *Colpoda* cysts (C) were stained with DAPI and PI and their nuclei were visualized by fluorescence via DAPI ('DAPI') and ('PI'), by a short-fix protocol ('S') or long-fix protocol ('L'). The scale bars of (A), (B), and (C) represent 30 μm, 30 μm, and 15 μm, respectively.
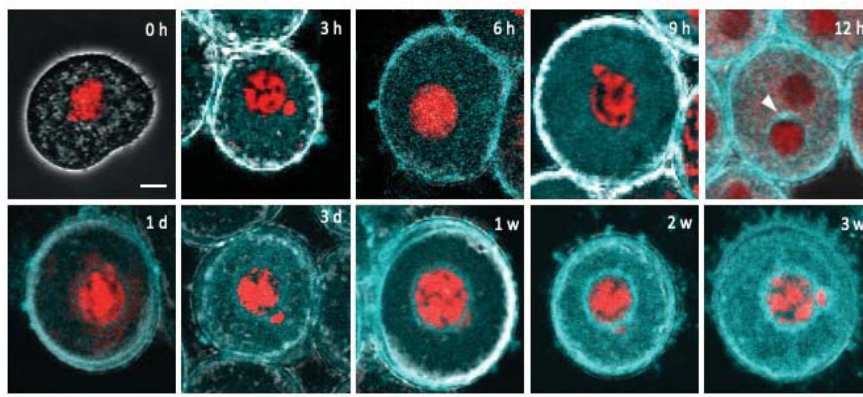
Fig. 4. Observations of NSPs with PI stained nuclei in vegetative cells '0 h' and cysts at 3 h, 6 h, 9 h, 12 h, 1 d, 3 d, 1 week, 2 weeks, and 3 weeks after the onset of encystment induction. The arrowhead of 12 h indicates NSP. The scale bar for vegetative cells is shown within the '0 h' image and for other samples it is shown on the bottom right of the entire figure. Each of them represents 10 μm.

Cyst-specific fluorescent structures such as lepidosomes and NSPs may contain a kind of pigment that perhaps absorbs the partial energy of radiation and might be responsible for antioxidant activity, as reported for *Deinococcus radiodurans*. The pigment deinoxanthin that was isolated from *D. radiodurans* (Lemee et al., 1997) was reported to be responsible for antioxidant activity (Carbonneau et al., 1989). If cells are irradiated by radiation rays such as ultraviolet or gamma rays, they can be damaged by reactive oxygen species (ROS) (Azzam et al., 2012). In this situation, their fluorescent materials protect the cells by absorbing some of the energy via scavenging to protect against radiation. The ability to tolerate radiation rays, including the activities of fluorescent materials, probably evolved to allow tolerance against desiccation for survival in terrestrial environments over long periods of time because ROS stress is also caused by desiccation (França et al., 2007).

CONFLICT OF INTEREST
The authors declare that they have no conflict of interest.

SUBMISSION DECLARATION AND VERIFICATION

This manuscript is approved by all authors and, if accepted, will not be published elsewhere in the same form, in English or in any other language, including electronically without the written consent of the copyright-holder.

REFERENCES

Akematsu T, Matsuoka T. 2008. Chromatin extrusion in resting encystment of *Colpoda cucullus*: a possible involvement of apoptosis-like nuclear death. Cell Biol Int. 32: 31–8.

Azzam EI, Jay-Gerin JP, Pain D. 2012. Ionizing radiation-induced metabolic oxidative stress and prolonged cell injury. Cancer Lett. 327: 48–60.

Benčaťová S, Tirjaková E. 2017. A Study on Resting Cysts of an Oxytrichid Soil Ciliate, Rigidohymena quadrinucleata (Dragesco and Njine, 1971) Berger, (Ciliophora, Hypotrichia), Including Notes on its Encystation and Excystation Process. Acta Protozool. 56: 77–91.

Benčaťová S, Tirjaková E. 2018b. Specific features of resting cysts morphology of limnic heterotrichous species ciliates *Blepharisma lateritium* and *Stentor roeselii*. Folia Faun Slovaca. 23: 21–27.

Carbonneau MA, Melin AM, Perromat A, Clerc M. 1989. The action of free radicals on Deinococcus radiodurans carotenoids. Arch Biochem Biophys. 275: 244–51.

Chessa MG, Largana I, Trielli F, Rosati G, Politi H, Angelini C, Corrado MD. 2002. Changes in the ultrastructure and glycoproteins of the cyst wall of *Colpoda cucullus* during resting encystment. Europ J Protistol. 38: 373–381.

Clement CG, Truong LD. 2014. An evaluation of Congo red fluorescence for the diagnosis of amyloidosis. Hum Pathol. 45: 1766–1772.

Foissner W. 1993. Colpodea (Ciliophora) Gustav Fischer Verlag, Stuttgart.

Foissner W, Muller H, Weisse T. 2005. The unusual, Lepidosome-coated resting cyst of *Meseres corliss*i (Ciliophora: Oligotrichea): Light and scanning electron microscopy, Cytochemistry. Acta protozool. 44: 201–215.

Funatani R, Kida A, Watoh T, Matsuoka T. 2010. Morphological events during resting cyst formation in the ciliate *Colpoda cucullus*. Protistology. 6: 104–217.

Funadani R, Sogame Y, Kojima K, Takeshita T, Yamamoto K, Tsujizono T, Suizu F, Miyata S, Yagyu KI, Suzuki T, Arikawa M, Matsuoka T. 2016. Morphogenetic and molecular analyses of cyst wall components in the ciliated protozoan *Colpoda cucullus* Nag-1. FEMS Microbiol Lett. 363: 203.

França MB, Panek AD, Eleutherio EC. 2007. Oxidative stress and its effects during dehydration. Comp Biochem Physiol A Mol Integr Physiol. 146: 621–31.

Gutiérrez JC, Callejas S, Borniquel S, Benítez L, Martín-González A. 2001. Ciliate cryptobiosis: a microbial strategy against environmental starvation. Int Microbiol. 4: 151–157.

Gutiérrez JC, Díaz S, Ortega R, Martín-González A. 2003. Ciliate resting cyst walls: A comparative review. Recent Res Devel Microbiol. 7: 361–379.

Izquierdo A, Martín-González A, Gutiérrez JC. 2000. Resting cyst wall glycoproteins isolated from two colpodid ciliates are glycine-rich proteins. Cell Biol Int. 24: 115-119.

Lemee L, Peuchant E, Clerc M, Brunner M, Pfander H. 1997. Deinoxanthin: A new carotenoid isolated from *Deinococcus radiodurans*. Tetrahedron. 53: 919–926.

Matsuoka T, Kondo A, Sabashi K, Nagano N, Akematsu T, Kida A, Ino R. 2010. Role of Ca^{2+} and cAMP in a cell signaling pathway for resting cyst formation of ciliated protozoan *Colpoda cucullus*. Protistology. 6: 103–110.

Matsuoka K, Funadani R, Matsuoka T. 2017. Tolerance of *Colpoda cucullus* resting cysts to ultraviolet irradiation. J Protozool Res. 27: 1–7.

Sogame Y, Kida A, Matsuoka T. 2011. Possible involvement of endocyst in tolerance of the resting cyst of *Colpoda cucullus* against HCl. African J Microbiol Res. 5: 4316–4320.

Sogame Y, Kojima K, Takeshita T, Fujiwara S, Miyata S, Kinoshita E, Matsuoka T. 2012a. Protein phosphorylation in encystment-induced *Colpoda cucullus*: localization and identification of phosphoproteins. FEMS Microbiol Lett. 331: 128–135.

Sogame Y, Kojima K, Takeshita T, Kinoshita E, Matsuoka T. 2012b. EF-1α and mitochondrial ATP synthase β chain: alteration of their expression in encystment-induced *Colpoda cucullus*. J Eukaryot Microbiol. 59: 401–406.

Sogame Y, Matsuoka T. 2013. Evaluation of intracellular Ca^{2+} concentration by fura 2 ratiometry in encystment-induced *Colpoda cucullus*. Acta Protozool. 52: 51–54.

Sogame Y, Kojima K, Takeshita T, Kinoshita E, Matsuoka T. 2014. Identification of differentially expressed water-insoluble proteins in the encystment process of *Colpoda cucullus* by two-dimensional electrophoresis and LC-MS/MS analysis. J Eukaryot Microbiol. 61: 51–60.

Sogame Y, Saito R, Koizumi R, Shimizu T, Ono T. Evidence of stress recovery in free-living ciliate *Colpoda cucullus*: The repair capability of resting cysts to damage caused by gamma irradiation. Acta Protozool. 58: 25–29.

Tamura K. 1992. Estimation of the number of nucleotide substitutions when there are strong transition-transversion and G+C-content biases. Mol Biol Evol. 9: 678–687.

Tamura K, Stecher G, Peterson D, Filipski A, Kumar S. 2013. MEGA6: Molecular evolutionary genetics analysis version 6.0. Mol Biol Evol. 30: 2725–2729.

Taylor CV, Strickland AGR. 1936. Effects of high vacua and extreme temperatures on cysts of *Colpoda cucullus*. Physiol Zool. 9: 15–26.

Uspenskaya ZI, Lozia-Lozinsky LK 1979. Antigen rearrangements in *Colpoda maupasi* cells after freezing at -196°C, and after shortwave ultraviolet irradiation. Cryobiology. 16: 542–549.

Venrni F, Rosati G. 2011. Resting cysts: A survival strategy in Protozoa Ciliophora. Ital J Zool. 78: 134–145.